MEASURING DYNAMICS OF SCATTERING CENTERS IN THE OCULAR FUNDUS

Luigi Rovati[a], Stefano Cattini[a], Francesco Viola[b] and Giovanni Staurenghi[b]
(a) Laboratory of Optoelectronics, Department of Information Engineering, University of Modena and Reggio Emilia, Via Vignolese 905, I-41100 MODENA, E-mail: luigi.rovati@unimore.it
(b) Department of Otorhinolaryngological and Ophthalmological Science
University of Milano, Via Tiraboschi 8, Milano, Italy I-20135 , E-mail: giovanni.staurenghi@unimi.it

Abstract- The study is focused on the analysis of the diffusing-wave-spectroscopy signal recorded in-vivo on the ocular fundus of a rabbit eye. The motion of the scattered sites was measured as a function of the pressure exerted by a Goldmann contact lens and during the moderate temperature increase induced by a therapeutic laser diode. Temporal fluctuations of the signal revel motion of molecules and thus changes in tissues temperature and chorioretinal blood velocity. Experimental results show the ability of the system to detect motion of the scattering sites in the ocular fundus layers during variations of the ocular pressure and laser heating.

Index terms*: Laser light scattering, diffusing-wave-spectroscopy, ocular fundus.*

I. INTRODUCTION

Dynamic light scattering (DLS) is a well-established technique to study the properties of the ocular tissues [1]. Several studies report its effectiveness in the early diagnosis of ocular pathologies [1]. Nevertheless, DLS has been proposed to analyze only the refractive ocular tissues since single-scattering regime is required. For ocular fundus tissues neither the diffusive-transport criteria nor single-scattering may be satisfied. To investigate these tissues the intensity temporal fluctuations should be integrated over the whole distribution of path lengths inside the medium. Diffusing-wave-spectroscopy (DWS) properly applied could extend conventional DLS to fundus tissues [2]. The standard DWS theory relies on the diffusion approximation, nevertheless recent studies extended the theory of DWS to multiple scattering regime where the ratio between photon path length and transport mean free path is in the order of few units [3].

Although DWS was first used to study molecules thermal motion in homogeneous media, later it was extended to include the cases of heterogeneities as well as shear and random flow.

An interesting feature of DWS is its ability to measure molecules motion, in a static matrix of tissue. Moreover, contribution of different layers can be recovered. According to Scheffold et al. [4], long delay time information can be associated with the short trajectories of photons, i.e. superficial layers. In fact, photons with long trajectories are completely decorrelated at long delay time, thus their contribution to the field autocorrelation function is not significant. The possibility of probing the dynamics of layered tissues was previously reported [5, 6].

In this study, we report DWS recordings on the ocular fundus of a rabbit eye. The paper first discusses the theoretical approach and the experimental methods used to investigate in-vivo the fundus tissues. Former, the study was carried out analyzing the effects of the ocular pressure exerted by a Goldman contact lens, and latter the effects of the thermal heating induced by a treating laser have been investigated.

II. METHODOLOGY

IIA. Theoretical Background

Photons migration through the ocular fundus is mainly governed by absorption and scattering phenomena, which are characterized by the absorption and reduced scattering coefficients μ_a and $\mu'_s = (1-g)\cdot\mu_s$. Here, μ_s and g are the scattering coefficient and the mean cosine of the scattering angle, respectively. The photon transport mean-free-path $l^* = (\mu_a + \mu'_s)^{-1}$ summarizes the absorption and scattering effects describing the average distance between migration events.

Ocular fundus tissues have been extensively studied by Hammer et al. [7], who reported in their paper the optical properties summarized in Table I.

Table I. Optical properties of bovine retina at 633 nm measured by Hammer et al. [7]

Tissue	μ_a (mm^{-1})	μ_s (mm^{-1})	g	μ'_s (mm^{-1})	l^* (mm)
Retina	0.25	25.00	0.97	0.75	1.00
RPE	90.00	120.00	0.84	19.20	$9.15\cdot10^{-3}$
Choroid	8.00	60.00	0.94	3.60	$86.20\cdot10^{-3}$
Sclera	0.25	80.00	0.9	8.00	$121.21\cdot10^{-3}$

Some of the absorbing and scattering centres in the ocular fundus tissues are rigidly fixed into the tissue structural matrix, whereas others can move. The motion of these centres is mainly thermally induced (Brownian) or due to the blood flow and depends on various parameters, i.e. shape and size of the molecules, interaction among other molecules, constraints due to membranes, and so forth. The molecules motion can be depicted in terms of dimensionless mean-squared displacement $\rho(\tau) = k^2 \left\langle \Delta r^2(\tau) \right\rangle$, where k is the wave number of light inside the tissue and $\left\langle \Delta r^2(\tau) \right\rangle$ is the mean-squared displacement of scattering sites at time τ [8].

Temperature induced motion is suitably described by the diffusion coefficient D_B of colloids, whereas blood flow in the choroidal capillaries can be described as a Gaussian random flow with mean square velocity $\left\langle v^2 \right\rangle$ [9].

Therefore, mean-squared displacement of the moving scatterers in the ocular fundus can be calculated as [5]:

$$\rho(\tau) = k^2 \left[\alpha \cdot \left(6 \cdot D_B \cdot \tau \right) + \beta \cdot \left(\left\langle v^2 \right\rangle \tau^2 \right) \right], \tag{1}$$

where α and β represent the probabilities that photons are scattered by a scattering site in Brownian motion or in random flow respectively.

When coherently illuminated, the moving scattering centers generate fluctuations of the scattered light intensity, which can be studied using the DWS theory. According to this theory, the normalized autocorrelation function of the scattered electric field is given by the average of the single-path correlation function weighted by the photon paths probability density P(s) [10]:

$$g_1(\tau) = \int_{\Gamma} P(s) \cdot e^{-\frac{\rho(\tau) \cdot s}{3 \cdot l^*(s)}} ds, \tag{2}$$

where Γ represents the space of all possible photon paths s.

In Eq. (1), we assume that scattering events and particle motions are uncorrelated, and that $l^*(s)$ is larger than the wavelength of light λ.

According to the approximations discussed in our previous paper [2], the dimensionless mean-squared displacement of the scattering sites can be easily calculated as:

$$\rho(\tau) = -\frac{3}{2} \cdot \gamma \ln\left(g_1(\tau)\right), \tag{3}$$

where γ depends on the photon path lengths through the ocular fundus and photon transport mean free paths reported in Table I.

To recover the function $g_1(\tau)$, a single mode fiber receiver can be exploited [11]. The normalized autocorrelation fluctuation of the scattered optical power collected by the receiver can be written as

$$g_2(\tau) = 1 + \frac{h}{\left(1+h\right)^2} \mathrm{Re}\left[g_1(\tau)\right] + \frac{1}{\left(1+h\right)^2} \left|g_1(\tau)\right|^2, \tag{4}$$

where heterodyne parameter h can be expressed as

$$h = \frac{J_s}{\left\langle J_d \right\rangle}. \tag{5}$$

J_s is the power of the static stray light which may be originated from backscattering by the scattering centres rigidly fixed into the tissue structural matrix, whereas $\left\langle J_d \right\rangle$ is the temporal average power of the light scattered by moving scattering centers. Note as that the classification of static and moving scattering centers depends on the observation time considered. If the incoherent background scattering can be neglected, the heterodyne parameter h can be determined from the initial value of the measured correlation function $g_2(\tau)$,

$$h = \frac{1}{g_2(0) - 1} - 1. \tag{6}$$

Since the measured $g_2(\tau)$ is subjected to noise, $g_2(0)$ is obtained by fitting the experimental data with a suitable smoothing function e.g., cumulant expansion.

Once the electric field autocorrelation function $g_1(\tau)$ has been calculated from Eq. (4), the dimensionless mean-squared displacement of the scattering sites is determined by means of Eq. (3).

IIB. System description and experimental methods

A block diagram of the developed system is reported in Fig. 1. We modified a commercial ophthalmic microscope (BQ900, Haag-Streit AG, Switzerland) equipped with the standard therapeutic laser diode LT (λ=810nm, Quantel Medical IRIDIS, France). Irradiation time and power were adjusted with the laser controller LC. The 70/30 beam splitter BS was used to couple probe beam and to collect the scattered light. A HeNe laser coupled to a single-mode fiber provided the illumination beam that was collimated by lens L1 and coupled to the ophthalmic microscope beam splitter BS. The resulting collimated beam was aligned to the microscope optics to be focused on the ocular fundus region of interest. Single-mode collection of scattered radiation was performed at a fixed distance from the illumination spot. Lens L2 focused this light into a second single mode fiber. To detect only the HeNe scattered light, the interference filter F was fixed in front of L2. Single photon counting module SPCM (AQR-14-FC, Perkin-Elmer, Québec, Canada) converted the scattered light intensity into an electrical signal that was processed by the digital correlator (FLEX99S160B, Correlator.com, USA). Figure 2a shows a picture of the beam splitter BS, coupled to the two single mode fibers. In the same picture the laser, the SPCM, the digital correlator and the PC are also visible. The whole measuring system including the therapeutic laser diode is shown in Fig. 2b.

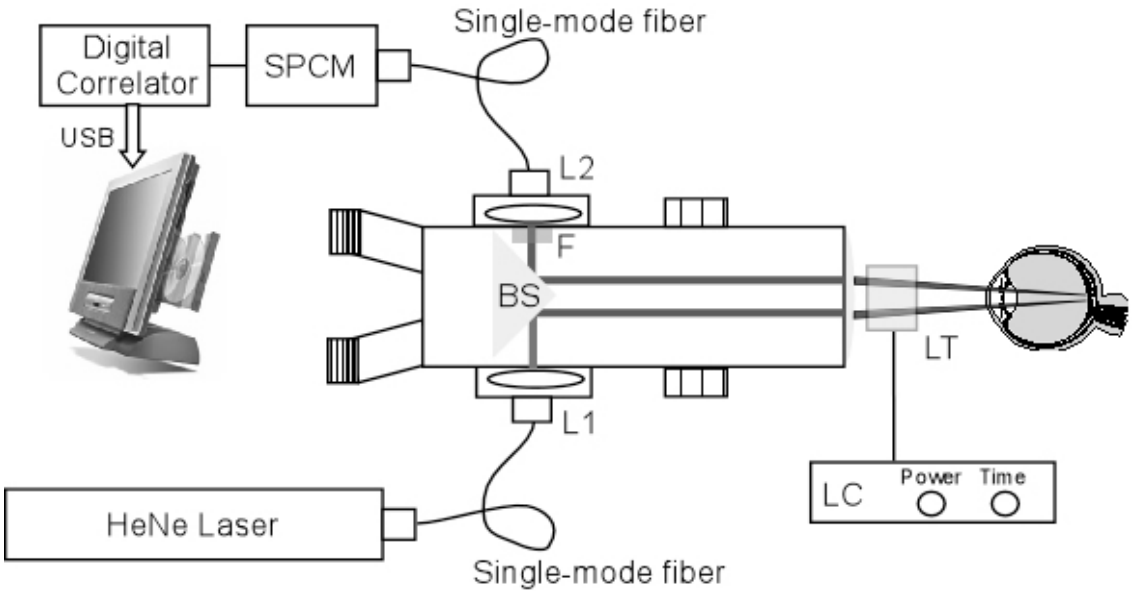

Figure 1. Block diagram of the system. L1 and L2: fiber coupling lenses, BS: 30/70 beam splitter, LT: NIR therapeutic laser, LC: therapeutic laser control, F: interference filter and SPCM: single photon counting module.

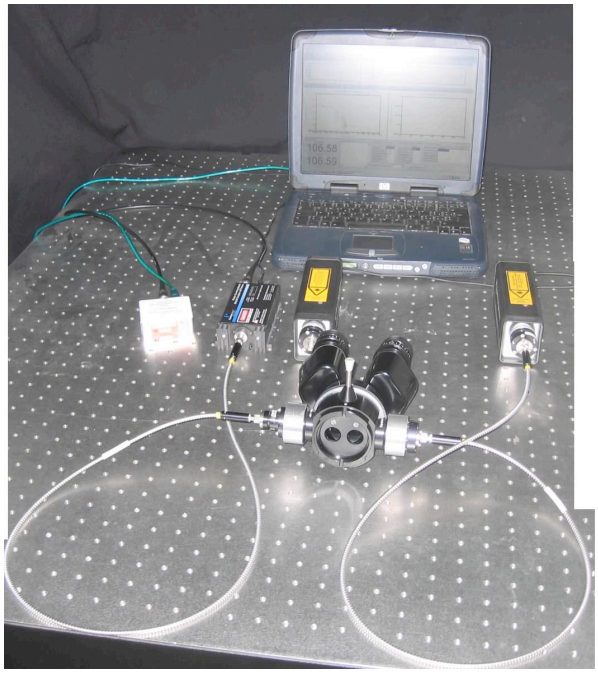

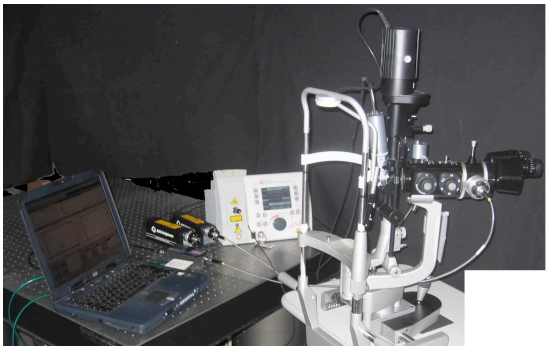

(a) (b)

Figure 2. Details of the measuring system (a) and whole measuring system including the therapeutic laser diode (b).

III. RESULTS

Experimental activity was performed on a pigmented rabbit fundus. The animal was anesthetized through intramuscular injection of ketamine (50 mg/kg; Ratiopharm, Ulm, Germany) and xylazine (3 mg/kg; BayerVital, Leverkusen, Germany). During the experiment, a Goldmann laser-coated contact lens was put on the rabbit cornea to make fundus observation easy by the microscope and to guide the treatment and probe laser radiation. The distance between illumination and collection spots was estimated to be about 2 mm. Values of photon paths lengths were calculated by considering the measuring geometry and the layers thickness of the rabbit fundus reported in literature [12]: retina, RPE and choroids thicknesses were set to 160 μm, 4 μm and 65 μm respectively. Thus constant γ in Eq. (3) has been calculated to be 0.165.

The motion of the scattered sites in the right eye fundus was varied performing two experiments:

i) exerting a pressure by the Goldmann contact lens;

ii) inducing a moderate temperature elevation by the therapeutic laser diode.

In both the experiments, DWS signals have been acquired in the inferior parapapillary region and the explored retinal region was chosen far away from visible vessels.

IIIA. Effects of the ocular pressure on the motion of the scattered sites

In the former experiment, an autocorrelation function was acquired before and after exerting the pressure by the Goldmann contact lens. Acquisition time of each autocorrelation function was 5 seconds. Figure 3(a) shows the two electric filed autocorrelation functions $g_1(\tau)$ acquired. The corresponding dimensionless mean-squared displacement functions of the scattering sites calculated according to Eq. (3) are reported in Fig. 3(b). Qualitatively, we can associate the long delay times information with the short trajectories of photons. In fact, photons with long trajectories are completely decorrelated at long delay times, thus their contribution to the field autocorrelation function is not significant [4]. Photons with short trajectories consist of the few photons travelling into the retinal layer without reaching the choroidal capillaries. On the other hand, the contributions at short delay times become from all the photons but the number of photons reaching the sclera is dominant, thus the rate of decrease of $g_1(\tau)$ is mainly determined by the mean-squared displacements of the scattering sites in the choroids. Fig. 3 shows as the

pressure exerted by the Goldmann contact lens changed mainly the mean-squared displacements of the scattering sites in the choroids. It is known that the choroids contributes 85% of the ocular blood flow thus as expected pressure tends to reduce the choroidal blood flow.

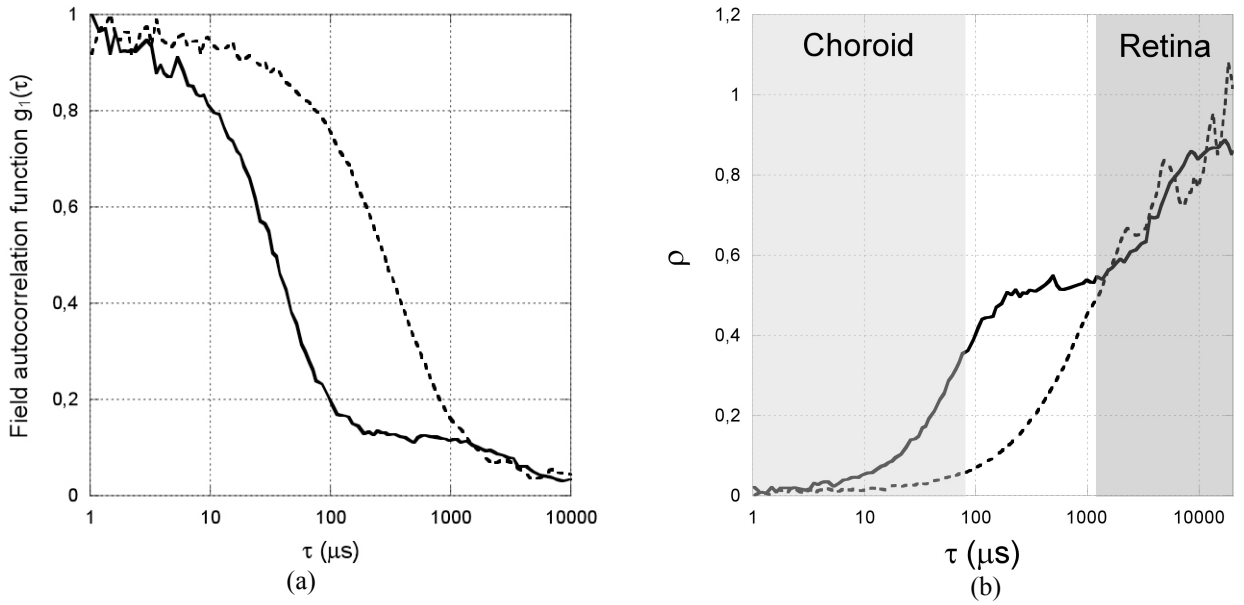

Figure 3. Field autocorrelation functions (a) and the corresponding dimensionless mean-squared displacements of the scattering sites (b) before (——) and after (---) exerting a pressure by the Goldmann contact lens.

Since the explored retina did not contain vessels, only thermal motion of scatteres was present (α=1), thus we fitted a linear function to $\rho(\tau)$ obtaining the slope $6 \cdot k^2 \cdot D_B$ in the retina delay range. We evaluated the diffusion coefficient D_B of the scatterers in the retina to be $1.65\ 10^{-8}\ \mathrm{cm}^2/\mathrm{s}$ before and $1.99\ 10^{-8}\ \mathrm{cm}^2/\mathrm{s}$ after exerting the pressure by the Goldmann contact lens. The slopes estimation showed as motion of the scatterers in the retina slightly increased as a consequence of the lens pressure elevation; this effect could be connected to different boundary conditions or optical properties of the layer.

In the choroids the photons probabilities α and β are unknown, thus in the short delay range we fitted a quadratic function to $\rho(\tau)$ obtaining the coefficient $6 \cdot k^2 \cdot \alpha \cdot D_B$ and the velocity parameter $k^2 \cdot \beta \cdot \langle v^2 \rangle$ related to the thermally induced and blood flow scatterers motions respectively. As a result, the diffusion coefficient and the Gaussian mean square velocity were calculated including the unknown coefficients α and β. We evaluated the diffusion coefficient

αD_B of the scatterers in the choroids to be $2373 \cdot 10^{-8}\ cm^2/s$ before and $259 \cdot 10^{-8}\ cm^2/s$ after exerting the pressure by the Goldmann contact lens, whereas the mean square velocity associated to the choridal random flow $\beta \cdot \langle v^2 \rangle$ was $0.075\ mm^2/s^2$ before and $0.023\ mm^2/s^2$ after exerting the pressure. Note as the pressure exerted by the contact lens mainly affected the motion of the scatterers in the choroids. Choroidal diffusion coefficient and mean square velocity exhibited a well-defined step-down in response to pressure elevation. Pressure induced vasodynamics of choroids is well known [13]. Our finding showed a large decrease in choroidal diffusion coefficient that can't be explained in terms of temperature variations. Nevertheless, the observed diffusion coefficient reduction could be induced by a restriction of the choroidal vasculature in response to the pressure elevation.

IIIB. Effects of the temperature on the motion of the scattered sites

In the second experiment, we induced a moderate temperature increase of the retinal tissues for 60 seconds using the near infrared therapeutic laser diode LT with a power setting of 200 mW (TTT: transpupillary thermotherapy). The aiming beam of the therapeutic laser was focused on the inferior parapapillary region; the treated area diameter was estimated to be about 4 mm. Immediately before TTT, an autocorrelation function was acquired in 5 seconds. Afterward, we started the laser thermal treatment. During the 60-second NIR laser exposure, an autocorrelation function was acquired each 10 seconds for a total of 6 readings. After the TTT, an additional autocorrelation function was acquired in 5 seconds. To exclude possible visible alterations of the tissues at the end of the treatment, an ophthalmologist observed the eye fundus.

As before, the mean-squared displacement functions in the retina and choroids delay ranges were calculated for all the acquired autocorrelation functions.

Thus, in the retina delay range, we fitted a linear function to $\rho(\tau)$ obtaining the slope $6 \cdot k^2 \cdot D_B$. The calculated diffusion coefficient D_B of the scatterers is shown in Fig. 4. The values of D_B at different stages of the experiment nicely showed as in the retina thermal motion of the scaterers increased monotonically during the TTT. According to the exponential fitting showed in Fig. 4, the time constant of the temperature trend was about 25 seconds in good agreements with temperature time scale heating reported by other researchers [14].

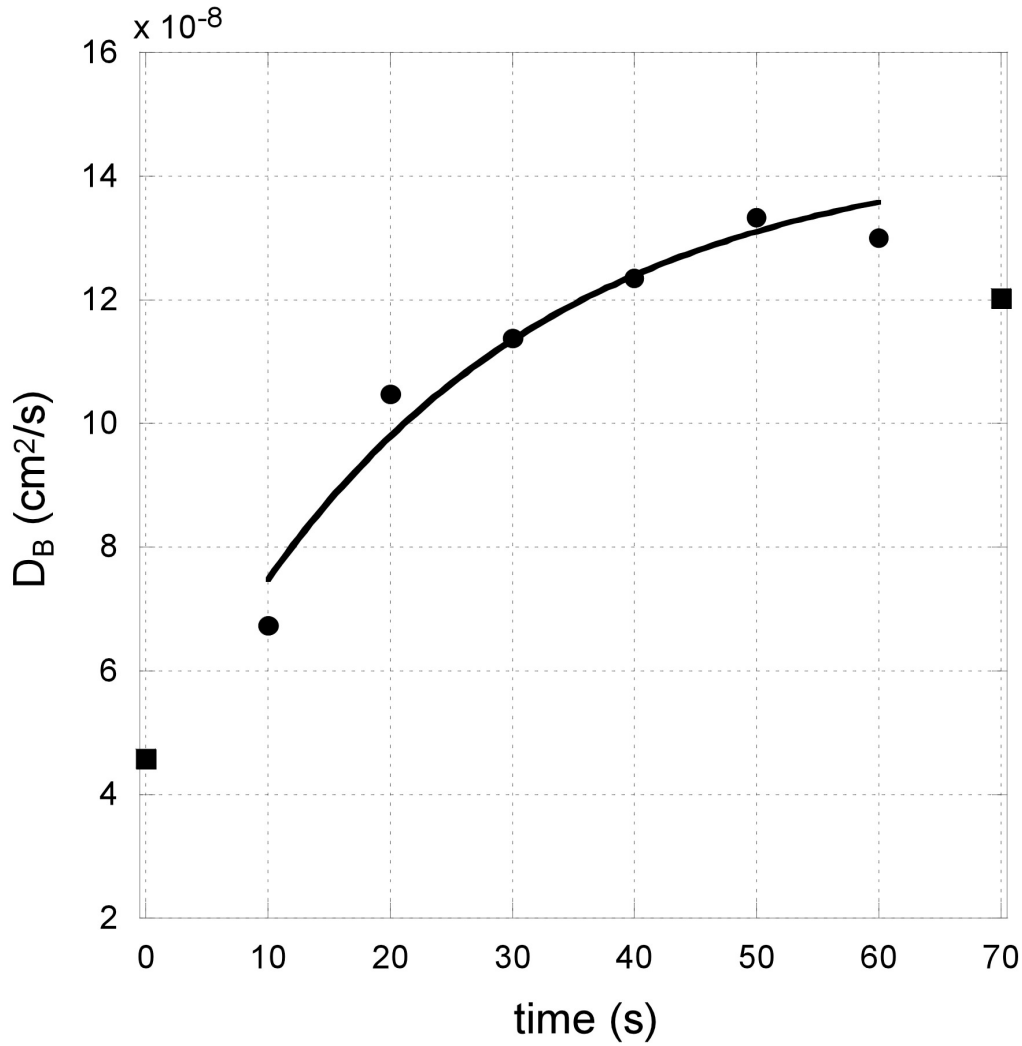

Figure 4. Diffusion coefficient of the scatterers in the retina immediately before and after TTT (■). The values of D_B acquired during the 60-second NIR laser exposure (●) showed as thermal motion of the scatterers increased monotonically during TTT. Bold line represents the best exponential fit of the experimental data acquired during the treatment.

As before, in the choroids delay range, we fitted a quadratic function to $\rho(\tau)$ obtaining the thermal motion coefficient $6 \cdot k^2 \cdot \alpha \cdot D_B$ and the blood velocity parameter $k^2 \cdot \beta \cdot \langle v^2 \rangle$. The diffusion coefficient and the Gaussian mean square velocity were calculated including the unknown coefficients α and β as reported in Fig.s 5(a) and 5(b).

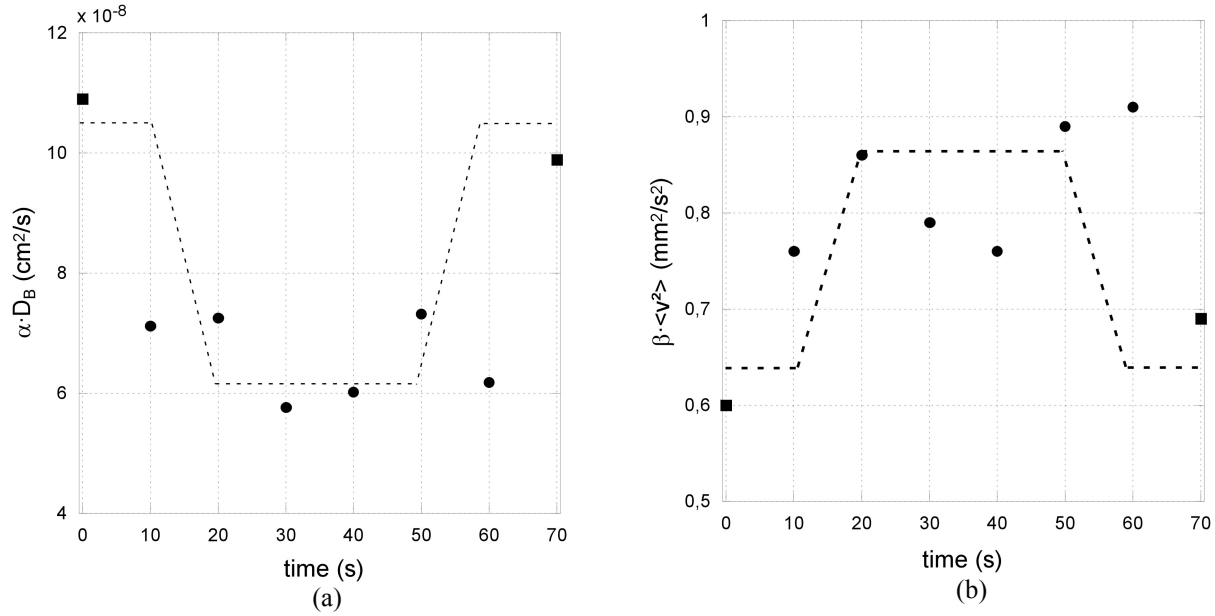

Figure 5. Diffusion coefficient (a) and Gaussian mean square velocity (b) of scatterers in the choroids. Data collected during the thermal laser treatment (●) and data collected before and after the treatment (■). The dashed curves are guide lines for the eye through the experimental points.

Choroidal diffusion coefficient exhibited a well-defined sharp step-down in response to the temperature elevation. This step reduction in the diffusion coefficient did not reflect the trend of temperature but different boundary conditions or optical properties of the scatterers. As shown in Fig. 5(b), we observed as the choroidal blood velocity upon heating of the fundus slightly increased.

It is known that choroidal blood flow can partially support heat dissipation during TTT, however if the increase of flow corresponds to an increase of blood volume, additional optical absorption due to hemoglobin could reduce the effects of the convection heat transportation. A recent human study showed as choroidal blood flow decreases upon heating of the eye [15]. This finding is mainly caused by the decrease in choroidal blood volume that suggests as choroidal vasculature may restrict in response to the increase in fundus temperature. This phenomenon could be confirmed by our observations in terms of reduction of the choroids diffusion coefficient.

Note as the above considerations do not take into account possible variations of the probabilities that the photons are scattered by a scattering sites in Brownian motion or in random flow, i.e. parameters α and β.

VI. CONCLUSIONS

A modified ophthalmic microscope has been developed to acquire in-vivo DWS signal from the eye fundus. Information concerning the motion of the scatterers in the fundus layers has been achieved. Much more work will be needed before DWS reaches clinical maturity, though these first results suggest that important diagnostic information can be extracted from in-vivo DWS measurements in the ocular fundus.

ACKNOWLEDGEMENTS

The authors wish to thank the Stella Major Foundation for the financial support to the research.

REFERENCES

[1] R.R. Ansari, "Ocular static and dynamic light scattering: a noninvasive diagnostic tool for eye research and clinical practice," J. Biomed. Opt. 9, pp. 22-37, 2004.

[2] L. Rovati, S. Cattini, N. Zambelli, F. Viola, and G. Staurenghi, "In-vivo diffusing-wave-spectroscopy measurements of the ocular fundus," Optics Express 15, pp. 4030-4038, 2007.

[3] A. Lemieux, M. U. Vera and D. J. Durian, "Diffusing-light spectroscopies beyond the diffusion limit: The role of ballistic transport and anisotropic scattering," Phys. Rev. E 57, pp. 4498-4515, 1998.

[4] F. Scheffold, S. E. Skipetrov, S. Romer and P. Schurtenberger, "Diffusing-wave spectroscopy of nonergodic media," Physical Review E 63, pp. 0614041-06140411, 2001.

[5] D.A. Boas, L.E. Campbell, A.G. Yodh, "Scattering and Imaging with Diffusing Temporal Field Correlation," Phys. Rev. Lett. 75, pp. 1855-1858, 1995.

[6] S.E. Skinpetrov and R. Maynard, "Dynamic multiple scattering of light in multilayer turbid media," Phys. Lett.A 217, pp. 181-185, 1996.

[7] M. Hammer, A. Roggan, D. Scweitzer and G. Müller, "Optical properties of ocular fundus tissue-an in vitro study using the double-integrating-sphere technique and inverse Monte Carlo simulation," Phys. Med. Biol. 40, pp. 963-978, 1995.

[8] D.A. Weitz and D.J. Pine, Dynamic Light Scattering: The Method and Some Applications (Claredon Press, Oxford,1993).

[9] A. Kienle, “Non-invasive determination of muscle blood flow in the extremities from laser Doppler spectra,” Phys. Med. Biol. 46, pp. 1231–1244, 2001.

[10] A.D. Gopal and D.J. Durian1, “Shear-Induced “Melting” of an Aqueous Foam,” J. Colloid Interface Sci. 213, pp. 169–178, 1999.

[11] L. Rovati, F. Fankhauser II and J. Ricka, "Design and performance of a new ophthalmic instrument for dynamic light scattering in the human eye," Rev. Sci. Instrum. 67, pp. 2615-2620, 1996.

[12] W.S. Weinberg, R. Birngruber and B. Lorenz, “The Change in Light Reflection of the Retina During Therapeutic Laser-Photocoagulation determined by histological examination,” IEEE J. Quantum Electron. QE-20, pp. 1481-1489, 1984.

[13] J.W. Kiel and W.A. van Heuven, “Ocular perfusion pressure and choroidal blood flow in the rabbit,” Invest. Ophthalmol. Vis. Sci. 36, pp. 579-585, 1995.

[14] J. Kandulla, H. Elsner, R. Birngruber and R. Brinkmann, “Noninvasive optoacoustic online retinal temperature determination during continuous-wave laser irradiation,” J. Biomed. Opt. 11, pp. 0411111-04111113, 2006.

[15] T. Nagaoka, and A. Yoshida, “The effect of ocular warming on ocular circulation in healthy humans,” Arch Ophthalmol 122, pp. 1477-1481, 2004.